

---

# MULTIMODAL OUTCOMES IN N-OF-1 TRIALS: COMBINING UNSUPERVISED LEARNING AND STATISTICAL INFERENCE

---

A PREPRINT

**Juliana Schneider**  
Hasso Plattner Institute  
Prof.-Dr.Helmert-Straße 2-3  
Potsdam, Germany  
juliana.schneider@hpi.de

**Thomas Gärtner**  
Hasso Plattner Institute  
Prof.-Dr.Helmert-Straße 2-3  
Potsdam, Germany  
thomas.gaertner@hpi.de

**Stefan Konigorski**  
Hasso Plattner Institute  
Prof.-Dr.Helmert-Straße 2-3  
Potsdam, Germany  
stefan.konigorski@hpi.de

September 14, 2023

## ABSTRACT

N-of-1 trials are randomized multi-crossover trials in single participants with the purpose of investigating the possible effects of one or more treatments.

Research in the field of N-of-1 trials has primarily focused on scalar outcomes. However, with the increasing use of digital technologies, we propose to adapt this design to multimodal outcomes, such as audio, video, or image data or also sensor measurements, that can easily be collected by the trial participants on their personal mobile devices.

We present here a fully automated approach for analyzing multimodal N-of-1 trials by combining unsupervised deep learning models with statistical inference. First, we train an autoencoder on all images across all patients to create a lower-dimensional embedding. In the second step, the embeddings are reduced to a single dimension by projecting on the first principal component, again using all images. Finally, we test on an individual level whether treatment and non-treatment periods differ with respect to the component.

We apply our proposed approach to a published series of multimodal N-of-1 trials of 5 participants who tested the effect of creams on acne captured through images over 16 days. We compare several parametric and non-parametric statistical tests, and we also compare the results to an expert analysis that rates the pictures directly with respect to their acne severity and applies a t-test on these scores. The results indicate a treatment effect for one individual in the expert analysis. This effect was replicated with the proposed unsupervised pipeline.

In summary, our proposed approach enables the use of novel data types in N-of-1 trials while avoiding the need for manual labels. We anticipate that this can be the basis for further explorations of valid and interpretable approaches and their application in clinical multimodal N-of-1 trials.

## 1 Introduction

With the increasing development and use of digital tools for personalized health recommendations, reliable methods for analyzing individual-level effects of different types of interventions for all kinds of health conditions are in demand. Patients and digital health consumers may wish to be able to easily and dependably assert the influence of a treatment, medication, or health intervention. A study design that has been on the rise for analyzing individual-level effects is N-of-1 trials [18]. N-of-1 trials are multi-crossover experimental studies in single participants, where an intervention or treatment and an alternative or baseline are alternated multiple times. The participants therefore serve as their own control. These trials are especially useful when the effect of a treatment can be assumed to vary between individuals so that there is no one-size-fits-all treatment, e.g. in the presence of comorbidities, but also in rare, chronic diseases or for expensive treatments where large-sample randomized controlled trials would not be feasible. Most work on N-of-1 trials so far has relied on numeric or binary outcome data such as self ratings or expert ratings that can be analyzed with standard statistical methods [25]. As mobile devices become more and more technologically advanced, the inclusion of

multimodal outcome data - audio, video, or images - might empower individuals to conduct their own trials on their mobile phones without the need for an expensive human expert evaluation of the health condition.

In recent work, we have published a first pilot multimodal N-of-1 trial in which five participants each conducted an N-of-1 trial alternating between using an acne cream (three of which used cream A, the other two cream B) and no intervention [8]. Typically, the severity of acne is measured by experts visually and involves the counting of pimples or lesions as well as overall skin irritation [2, 11, 28]. Whereas the former is numeric information that can easily be established from an image, the latter is more subjective. Possible indicators for irritation could be redness of the skin or the (average) size of the pimples. A holistic consideration of all characteristics and changes in the skin might thus improve the detection of treatment effects on acne. While there are many studies using deep learning models on multimodal data, to the best of our knowledge the study by Fu et al. [8] is the first and only study that has incorporated multimodal data as outcomes in N-of-1 trials. For example, with respect to skin conditions, few N-of-1 trials have been performed at all and further none of the published studies directly used visual changes as measurements but rather physical markers or rating scales as outcome variables [3, 10, 17, 26]. One study examined two alternative methods for wound closure by visual review and scoring [15]. The trials in the multimodal acne N-of-1 trial [8] lasted 16 days in total, with 3 measurements per day, two days each of intervention and non-intervention phases in an alternating design. The study resulted in a total of 255 images over all participants and tested treatment effects using a t-test based on a CNN-based model trained on the manual labels. While the approach was successful in identifying a treatment effect in one participant, the approach required manual labeling of the images, which is not feasible for a large-scale deployment of such trials [8].

In this study, we propose an automated unsupervised approach that is able to analyze multimodal N-of-1 trials without the need for expert labeling. The unsupervised learning approach first finds lower dimensional representations of the images, on which statistical tests are applied subsequently to test treatment effects. By training an unsupervised model, labels for each image do not need to be provided any longer. The analysis is then based on the assumption that the embeddings obtained from the unsupervised learning capture the relevant features in the input images, so that can then be used to identify a difference between intervention and non-intervention phases. The approach is tested on published trial data testing whether a skin cream has an effect on acne.

The manuscript is structured as follows: In the sections 2 and 3, we present our proposed approach: The data is fed into an *Autoencoder* (AE), then reduced to univariate values in a *Principal Component Analysis* (PCA) so that we can lastly run classical statistical tests with high interpretability on the results. For illustration, we use the acne trial throughout in the description and application of our proposed approach. The results are described in section 4 and show an effect in the same individual as in the baseline rating. Lastly, we discuss possible shortcomings and further steps in section 5.

## 2 Methods

### 2.1 Overview

The overall aim of this work is to provide a framework for automatically identifying effects of one or more treatments on an outcome from unstructured data such as images, where no labels are provided. For the aim of using images directly as outcome data, we need to train a model that can find meaningful embeddings that capture the relevant features in the image, in our case meaningful features of acne on the skin. Unsupervised learning approaches can be used in this setting to compress relevant information of an image in  $n$ -dimensional space. There is a variety of available unsupervised approaches, which differ not only in their architecture but also in their training methods. For instance, pretrained models could be fine-tuned for the specific task at hand, or a proxy-learning task may enhance the power of a model.

Here, we use a two-step approach to represent the image in one value. First, we choose an AE model to embed the images in a lower-dimensional embedding space to capture the relevant features of acne severity in an unsupervised fashion. AEs can represent complex information in the embedding space and can be trained without label. Second, we use PCA to reduce the dimensionality of the embeddings to one scalar per image, which can be used for statistical testing. Then, we apply various univariate tests such as a linear model with *First order autoregressives* (AR1s) error structure and randomization tests to test the null hypothesis of no difference in outcomes between intervention and non-intervention phases. See Figure 1 for an illustration.

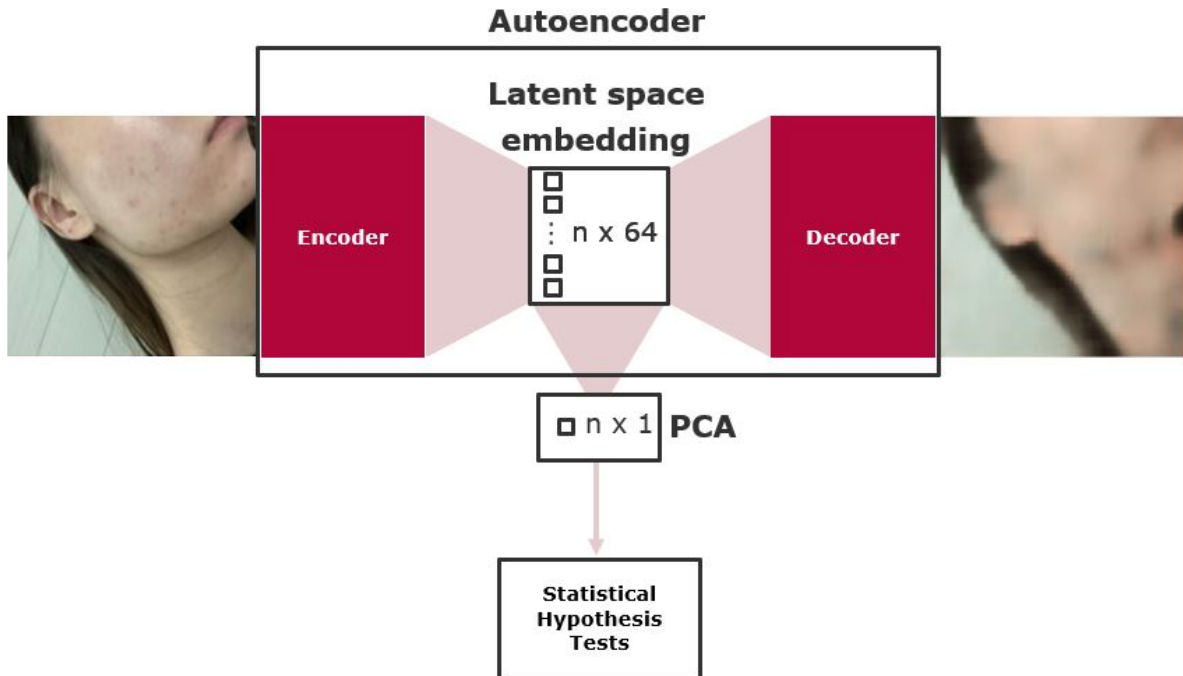


Figure 1: Illustration of the three steps - unsupervised learning, dimensionality reduction, statistical inference - of the proposed approach.

## 2.2 Step 1: Unsupervised learning to obtain embeddings of outcomes

### 2.2.1 Autoencoder

In this approach to integrate multimodal data in N-of-1 trials, we used autoencoders as an efficient tool to learn lower dimensional representations of an input. Autoencoders consist of two deep models: an encoder capturing the features of an input - here, an image - and a decoder that is fed the latent space vectors from the encoder to reconstruct the input [9]. By transforming the original input, the autoencoder maps into a lower dimensional space and can therefore create efficient nonlinear, possibly correlated representations. The encoder poses a bottleneck for the decoder, as it aims to represent the input efficiently and capture relevant features, while not creating exact copies [9]. Since we deal with relatively few data points in typical N-of-1 trials, this bottleneck property may help with accurately embedding the input features. The restored images provide a visual heuristic to evaluate the quality of the embeddings.

In a bit more detail, autoencoders comprise two functions:

$$\begin{aligned} T &= G(Y) \\ Y' &= H(T) \end{aligned} \tag{1}$$

where  $Y$  is the input image,  $G(\cdot)$  an arbitrarily complex mapping function into the latent space,  $T$  the latent space embedding, and  $H(\cdot)$  a mapping function to restore the input,  $Y'$ , with the aim of minimizing the distance between  $Y$  and  $Y'$  [16]. Thus,  $G(\cdot)$  represents the encoder part and  $H(\cdot)$  represents the decoder part of the model.

In this study, we specified the loss for the two-stage optimization problem as the sum of the reconstruction error, i.e. the mean squared error between reconstructed and original image: [16]

$$L = \frac{1}{n} \sum_{i=1}^n (Y_i - Y'_i)^2, \tag{2}$$

where  $i = 1, \dots, n$  denotes the images (for which, in our case the images of all participants are used in training). As a result of the autoencoder, we extract the  $k$ -dimensional latent embedding.

### 2.2.2 Principal Component Analysis

*Principal Component Analysis* (PCA) is a popular technique for dimensionality reduction. It performs an orthogonal linear transformation of high-dimensional input data that can be used to project into a lower dimensional space while maintaining as much variation of the original data as possible. Let  $n$  be the number of images and  $k$  the dimensionality of the latent variables in the embeddings in the autoencoder. Then with PCA, we linearly transform the  $k$  latent variables  $X_1, \dots, X_k, \mathbf{X} \in \mathbb{R}^{n \times k}$ , into a single new variable  $t = \mathbf{X}\omega$  with the aim of maximizing  $var(t)$  over  $\|\omega\| = 1$ . Here,  $\|\cdot\|$  is the Frobenius norm, since arbitrarily large  $\omega$  would result in an arbitrarily large  $var(t)$  [5]. Principal components are the eigenvectors of the input's covariance matrix, and as such can be computed by eigenvalue decomposition or singular value decomposition [13]. Thus,  $var(t) = var(\mathbf{X}\omega) = \omega' \mathbf{S} \omega$ , where  $\mathbf{S}$  is the variance-covariance-matrix of  $\mathbf{X}$ . The maximization problem then can be rewritten as:

$$\arg \max_{\|\omega\|=1} \omega' \mathbf{S} \omega - \lambda(\omega' \omega - 1),$$

where  $\lambda$  is the Lagrange multiplier. Differentiating and solving with respect to  $\omega$  yields that  $\omega$  is the eigenvector and  $\lambda$  the corresponding eigenvalue of  $\mathbf{S}$ . In our approach, the dimensions of the embeddings from the autoencoder serve as the columns of the input data for the PCA. Accepting a loss of information, we extract only the first principal component to enable direct use of classical statistical tests and a direct comparison to the analysis of the average scores provided in the study of Fu et al. [8].

### 2.3 Step 2: Statistical inference on treatment effects with embeddings

In the second step, we wish to use the embeddings generated from the input images as outcomes in classical statistical tests. Classical statistical tests provide a straightforward interpretation. Interpretability is especially useful when working directly together with clinicians or patients. Depending on the exact tests, conclusions about statistical significance, direction and even magnitude of an effect can be drawn. Such tests may be as simple as t-tests, linear models, or randomization tests. However, they do not capture time dependencies between data points, which is why when using ordinary least squares (OLS) models, we incorporated lagged variables of lag 1 as predictor variables.

#### 2.3.1 T-Test

A paired t-test compares the difference of expected values of two groups  $X$  and  $Y$  from the same population. Let  $I$  be an indicator variable for intervention which is 1 under treatment and 0 under no treatment, and  $PC$  as the outcome represented as the *Principal Component* (PC) score resulting from the AE's embeddings. Then the null hypothesis for the t-test in the acne trial is  $H_0 : E(PC|I = 1) = E(PC|I = 0)$  and the test statistic is

$$t = \frac{\sum_{i=1}^n D_i}{\sqrt{\frac{n(\sum_{i=1}^n D_i^2) - (\sum_{i=1}^n D_i)^2}{n-1}}}, \quad (3)$$

where we set  $D_i = PC_{i,I=1} - PC_{i,I=0}$  as the difference in means between intervention and non-intervention phases. Here,  $i$  is the  $i$ th observation of  $n$  total observations in either intervention or non-intervention phases. We assume in this case that there is an equal number of observations between  $PC$  scores for intervention and non-intervention phases, i.e.  $n_{I=1} = n_{I=0}$ .

#### 2.3.2 Linear Model with AR1 error structure

*Linear Models* (LMs) are a standard means in N-of-1 trials to assess the influence of a treatment on an outcome of interest [25, 27]. An advantage of LMs is that they can incorporate influences of covariates. The general model equation is:

$$PC_t = \beta_0 + \beta_1 I_t + \epsilon_t, \quad (4)$$

where  $PC_t$  is defined as the resulting Principal Component at time point  $t$ . The null hypothesis for the LM in the acne trial is then  $H_0 : \beta_1 = 0$ . We assume that the error-term  $\epsilon_t$  is following a first-order autoregressive (AR1) structure with  $\epsilon_t = \rho \epsilon_{t-1} + \varepsilon_t$  and  $\varepsilon_t \sim \mathcal{N}(0, \sigma^2)$ . Incorporating an AR1 error structure acknowledges the time dependence of the measurements in a single-person trial [1]. The structure is such that the covariance between the errors decreases towards zero with increasing lag.

### 2.3.3 (Single-Case) Randomization Tests

As a non-parametric approach, permutation tests can be performed to test for treatment effects on N-of-1 trial outcomes. In permutation tests for two groups - i.e. intervention and non-intervention or alternative - the realized partition of outcome values to the two groups are compared to all possible partitions and then the p-value of the realized outcome is calculated. If data of sample size  $N$  can be randomly split into two groups of sizes  $n$  and  $m$ ,  $\binom{N}{n}$  assignments to the two groups are possible [7].

Permutation tests test one of three hypotheses:

1. The realized value stems from the same distribution and has been assigned randomly to the two groups.
2. If the values are assumed to be paired between the groups, the order of the pairs is random.
3. If the values are assumed to be paired between the groups, the assignment to the groups is random, i.e. the groups of a pair could be swapped.

In N-of-1 trials, the according randomization test would test the hypothesis that the outcome data from intervention and non-intervention phases within one person stem from the same distribution [12], which corresponds to hypothesis type number 1 above. In other words, the null hypothesis tested is that there is no mean difference between intervention and non-intervention phases [4]:  $H_0 : E(PC_i|I = 1) = E(PC_i|I = 0)$  for all permutations  $i = 1, 2, \dots, n$ . Still, it is necessary to take into account the order of the phases within a person's trial, since the data are not independent. Thus, in a *Single-Case Randomization Test* (SCRT), the realized ordered outcome of the trial at hand (i.e. the order of treatment and non-treatment phases and their respective outcome values) is compared to all possible orders of assignments of treatment and non-treatment in a trial of the same length. [19].

Afterwards, the test statistic of interest for the realized trial is computed. In the case of our study,  $E(PC|I = 1) < E(PC|I = 0)$  is estimated, as the acne cream is supposed to lower the score on an acne severity scale. The realized statistic is now compared to the distribution of all possible assignments of the values to them and their respective p-value,  $p$ , computed. Now, the p-value for the randomization test is calculated as follows:

$$p = P(S \leq s^* | H_0) = \frac{\sum_{i=1}^{\binom{N}{n}} I(s_i \leq s^*)}{\binom{N}{n}}, \quad (5)$$

where  $s_i$  is the value of the test statistic  $s_i = \bar{PC}_{i,I=1} - \bar{PC}_{i,I=0}$  for the  $i$ th of  $n$  randomizations,  $I(\cdot)$  is the indicator function, and  $s^*$  is the observed value for  $s$ . Since computing all possible  $\binom{N}{n}$  permutations may be infeasible with larger  $N$ , Monte-Carlo sampling from the randomization distribution poses a slightly less efficient, but equally exact estimate of the p-value,  $\hat{p}$ . With  $M$  samples, the estimate would then be, following Ernst [7]:

$$\hat{p} = \frac{1 + \sum_{i=1}^M I(s_i \leq s^*)}{M + 1} \quad (6)$$

The advantage of randomization tests is that they do not rely on strict assumptions of Normality, such as the t-test. Moreover, the specific advantage of the Single-Case Randomization Test by Onghena et al.[12, 20] over regular randomization tests is that it takes into account the structure of single-case designs, in this case, an ABAB-design.

## 3 Experimental Setup

### 3.1 Data

For the illustration of our proposed approach, we used the published multimodal N-of-1 trial data on acne ([https://github.com/HIALab/Multimodal\\_Nof1/tree/main/Data/Acne\\_Nof1\\_trial](https://github.com/HIALab/Multimodal_Nof1/tree/main/Data/Acne_Nof1_trial)). Here, five participants conducted a series of N-of-1 trials alternating between using an acne cream (three participants used cream A, the other two participants cream B) and no intervention. The trials lasted 16 days in total, with 3 measurements per day, intervention and non-intervention phases of two days each, in an alternating design. The study resulted in a total of 255 images for all participants. The images were taken in a standardized setting with fixed rooms, lighting, and position as well as the same phone every time. Additionally, temperature at the time of taking the image, application of lotion or make-up, and a treatment indicator were registered.

Each image was scored blindly by 5 students in terms of acne severity, which was standardized on a scale between 0 and 1, and averaged afterward. These scores serve as a baseline reference for our proposed unsupervised approach. In [8], results from a t-test on a CNN-based model trained on the manual labels were reported, and an effect of the acne treatment was found for the patient with ID 2.

### 3.2 Step 1: Unsupervised learning

The pipeline was constructed with the following steps: First, the input images were preprocessed and augmented using standard approaches: horizontal flips, increase of color brightness, and a resizing to (224,224). Next, an autoencoder was trained with a batch size of 32 and consisted of 7 convolutional layers and a linear output layer each with ReLU in the encoder, yielding the final 64-dimensional output embeddings. The decoder consisted of 1 linear and 5 pairs of convolutional layers and transposed convolutional operators and ReLU activation with a sigmoid function in the end. See a schematic depiction of the AE in Figure 2. The AE was then trained for 10 epochs with a learning rate of 0.001, using Adam as optimizer. We specified the loss as the reconstruction error, i.e. the Mean Squared Error between reconstructed and original image. Due to the limited amount of data, we forwent a train-test-split, instead using an augmented version of the input images as train and a differently augmented version with a random horizontal flip of 0.5 probability - all else equal - as validation set.

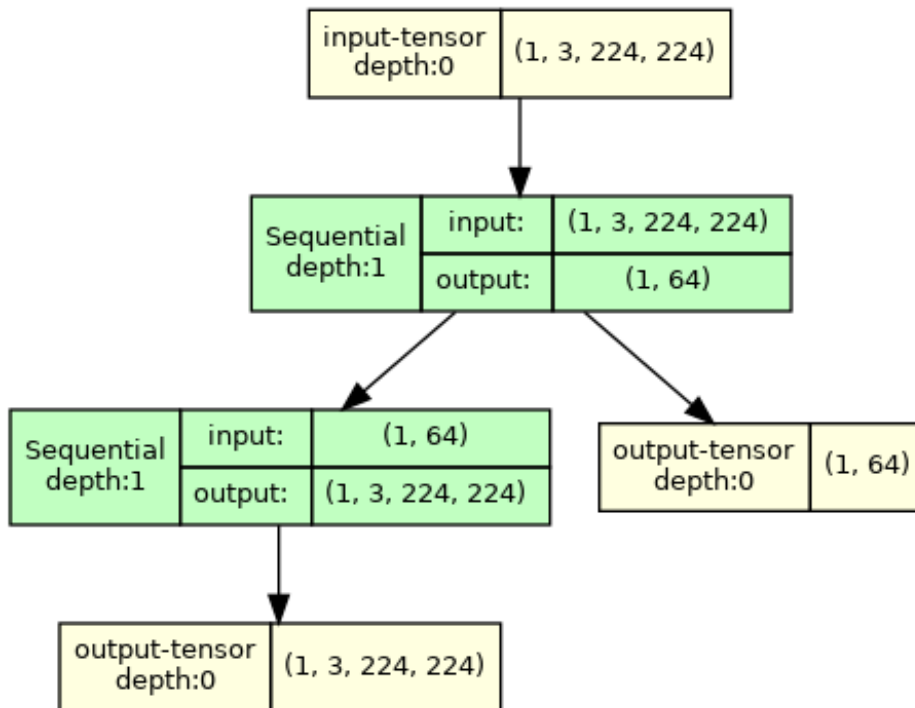


Figure 2: Model architecture of the autoencoder.

Afterwards, the 64-dimensional output vectors were run through a PCA, and the first PC was extracted to reduce the data to a single component comparable to the self-rated daily average scores. The resulting PC scores were used in the various hypothesis tests outlined in subsection 2.3. All these steps were performed in python. In particular, all embeddings including data augmentation were created using pytorch [21]. For the PCA, sklearn [22] was used.

### 3.3 Step 2: Statistical inference

Now, we applied the different statistical tests described in section 2.3 on the PC scores as well as for the average scores for each ID, respectively. The t-tests were computed using `scipy.stats` [29] in python. The LM with AR1 error structure was fitted using the library `nlme` [23] in R with default settings. Finally, we tested different randomization tests. SCRT is the randomization test developed for single case experimental designs described in section 2.3.3 and was computed using the library SCRT [6] in R. In addition, we evaluated permutation tests available in the `scipy` [29] and `mlxtend` [24] packages in python which are not specific to single case designs. These two implementations test whether the values from the intervention and non-intervention phases were drawn from the same distribution, without

taking into account the ABAB-structure in the data. Instead, they treat the phases as in a regular crossover trial. In the case of both SCRT and `scipy` permutation tests, we tested the null hypothesis that the expected value of the outcome under treatment  $A$  is larger than under treatment  $B$   $\mu_A - \mu_B$ , i.e.  $\mu_{O_{I=0}} - \mu_{O_{I=1}} > 0$ , or  $\mu_{O_{I=0}} > \mu_{O_{I=1}}$ , where  $\mu_{O_{I=1}}$  describes the expected value of the outcome, when the patient was exposed to the treatment and  $\mu_{O_{I=0}}$  when the patient was not exposed respectively. In the case of `mlxtend` permutation tests, we tested the hypothesis  $\mu_A < \mu_B$ , i.e.  $\mu_{O_{I=0}} < \mu_{O_{I=1}}$ . P-values were obtained and compared subsequently.

## 4 Results

### 4.1 Autoencoder

The training loss for the autoencoder after 10 epochs was 0.031. The test loss after 10 epochs was 0.027. A visual comparison of original and reconstructed images showed blurry results. Beige colors and shading were recognizable (see Figure 3). This is a common occurrence in likelihood based generative models, which often lead to blurry reconstructed images. So while the reconstructions were not of the highest quality, it can still be assumed that the embeddings have captured meaningful information about the images.

### 4.2 PCA

The first principal component explained 98.2 % of variance in the embeddings. Its values ranged from -4.39 to 6.37 with 255 unique values in total (see Table 1).

ID	Intervention	Average Score			PC Score		
		min	max	mean	min	max	mean
1	No	0.0	0.8	0.42	-2.93	0.62	-1.50
	Yes	0.0	0.9	0.54	-3.07	1.76	-1.32
2	No	0.2	1.0	0.54	-1.81	6.39	0.86
	Yes	0.1	0.7	0.36	-1.10	2.10	-0.15
3	No	0.1	0.9	0.46	-2.50	6.37	1.25
	Yes	0.0	0.9	0.43	-1.07	3.60	1.20
4	No	0.0	0.9	0.34	-0.69	6.19	2.20
	Yes	0.1	0.9	0.37	-1.00	5.72	1.91
5	No	0.1	0.9	0.52	-4.39	0.22	-2.93
	Yes	0.1	0.8	0.48	-4.20	0.47	-2.54

Table 1: Ranges and means of the Average and PC scores stratified by User ID and Intervention.

### 4.3 Descriptive statistics

The values for average score ranged from 0.0 to 1.0 with means between 0.45 and 0.50 for all IDs except for ID=4 with the lowest mean average score of 0.35. The means between non-intervention and intervention phases increased for ID=1 and ID=4 and decreased for ID=2, ID=3 and ID=5. The means of the PC scores between IDs differed largely, from -2.73 for ID 5 to 2.07 for ID 4. The means between non-intervention and intervention phases decreased for ID=2 and were very similar for all other 4 participants. Whereas ID=4 had the lowest overall mean average score of 0.35, the participant had the highest overall mean PC score of 2.07. ID=5 showed an opposite pattern, with the highest overall mean average score of 0.50 but the lowest overall mean PC score of -2.73. See Table 1 for more details.

In Figure 4, the time series for the average score and the PC values are shown for each ID. Both time series do not seem to follow similar patterns over time. Also, the scores between intervention and non-intervention phases, colored in blue and orange, respectively, show visual differences among the plots.



Figure 3: Original (left) and reconstructed (right) images.



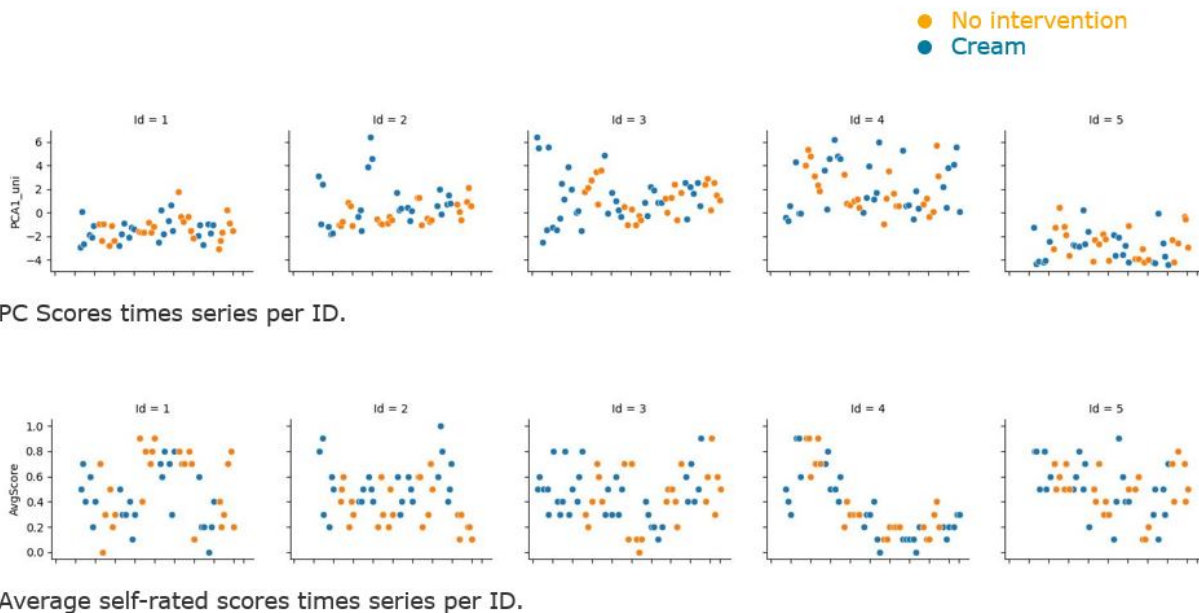


Figure 4: Time series plots per ID for average scores and PC scores. Non-intervention phases are highlighted in orange, intervention phases are highlighted in blue.

#### 4.4 Hypothesis tests

Table 2 shows the results of the different hypothesis tests. The baseline t-test, the randomization tests SCRT and MLX *Randomization Test* (RT) all identified a treatment effect for ID=2 with p-values  $< 0.05$ . These findings mirror the original study that had identified ID=2 with a p-value smaller than 0.05 as well. The p-value of the Wald test of the regression coefficient for intervention in the LM with AR1 error structure was not significant, although it produced the lowest p-value for ID=2 compared to all other IDs. These results suggest that randomization tests seem well-suited to test effects on embedding-based PC scores. T-tests are quite robust against violations of their assumptions and might therefore also have produced a significant result for ID=2, while the autoregressive linear model did not.

Test / ID	1	2	3	4	5
<b>t-test</b>	0.551	0.034	0.918	0.612	0.318
<b>LM AR1</b>	0.281	0.092	0.824	0.501	0.473
<b>SCRT</b>	0.770	0.000	0.699	0.456	0.749
<b>Scipy RT</b>	0.661	0.060	0.752	0.928	0.439
<b>MLX RT</b>	0.635	0.044	0.614	0.538	0.734

Table 2: P-values of the statistical tests per ID.

## 5 Discussion

In this work, we present an approach that combines unsupervised learning with statistical inference for an automated analysis of multimodal outcome data in N-of-1 trials. For this, we trained an autoencoder to create efficient embeddings of input images of an acne N-of-1 trial that were subsequently reduced to one dimension through PCA and tested for their association with acne cream treatments. We compared these findings with the average of the self-reported scores from the five study participants. The average score identified a statistically significant treatment effect of acne cream for one study participant, which was reproduced by our proposed unsupervised approach. This indicates that our unsupervised approach can be successful in mirroring the results of supervised approaches, which require manual expert labeling with supervised models and are not applicable on a wider scale of N-of-1 trials. In a more detailed inspection of our results, it showed that in the comparison of different statistical tests and different implementations, only the t-test and randomization tests identified a treatment effect while the linear model with AR1 error structure yielded a p-value

of 0.092. Sensitivity analyses suggest that the residuals did not follow an AR1 structure but only showed a very small dependence, so that using this misspecified model might have yielded the small observed efficiency loss.

Based on our proposed approach here, there are several opportunities for improvement and follow-up work. First, for training of the autoencoder, we used standard hyperparameters and image augmentation techniques. More sophisticated hyperparameter or architecture tuning may improve the reconstruction results. Furthermore, other models such as variational autoencoders might also yield more meaningful embeddings. Similarly, more elaborated hypothesis tests could be used to incorporate time-dependencies, the influence of covariates, and carryover adequately to test complex effect differences between intervention and non-intervention phases. Second, when training deep models, the amount of training data available is important in order to train a good model, in our case here be able to extract meaningful features in the embeddings of the autoencoder. Depending on the specific N-of-1 trial, suitable openly available datasets for pretraining or proxy-task training of a model to later be fine-tuned on the trial data may be helpful. Third, not only the amount, but also the quality of data is important. The baseline average score for this study could be improved by collecting more ratings from a larger group of experts (or non-experts, e.g. from more students than the initial five) to reduce variance and increase inter-rater-reliability. Furthermore, acne scoring methods based on severity and number of lesions on the skin, as have been developed already and are used by dermatologists, may help generate reliable labeled data or be used as a training task for the model. Fourth, for simplicity of the presentation and in order to compare the results to the analysis of expert-derived average acne scores, we first created a 64-dimensional embedding layer and then extracted one dimension from the latent embedding with PCA. As another possibility, the dimensionality out the outcome could be reduced to one dimension as well by pushing the AE to compress the input to one-dimensional embeddings. Other dimensionalities of the latent space may yield better results, or other dimension reduction methods such as tSNE could be employed. As another possibility, the PCA does not need to be restricted to only one factor, and could be skipped entirely by performing multivariate hypothesis tests such as proposed in [14]. Lastly, further investigations into the meaningfulness of the embeddings given the low amount of data in a single N-of-1 trial could lead to improved models. As of now, it is still an open question how the meaningfulness of the latent space could be assessed. We suggest different types of visualizations and comparisons with trusted baseline results or simulation studies.

In summary, our approach serves as a first valuable step towards incorporating unsupervised models on multimodal outcome data in N-of-1 trials. It is a contribution towards more accessible and comprehensive personalized interventions that may serve a broader population in the future.

## References

- [1] The state of the art and future opportunities for using longitudinal n-of-1 methods in health behaviour research: A systematic literature overview. <https://www.tandfonline.com/doi/epdf/10.1080/17437199.2017.1316672?needAccess=true&role=button>.
- [2] Tamara Agnew, Gareth Furber, Matthew Leach, and Leonie Segal. A Comprehensive Critique and Review of Published Measures of Acne Severity. *The Journal of Clinical and Aesthetic Dermatology*, 9(7):40–52, July 2016.
- [3] D.F. Arnold, J. Burton, B. Shine, F. Wojnarowska, and S.A. Misbah. An ‘n-of-1’ placebo-controlled crossover trial of intravenous immunoglobulin as adjuvant therapy in refractory pemphigus vulgaris. *British Journal of Dermatology*, 160(5):1098–1102, May 2009.
- [4] Samantha Bouwmeester and Joran Jongerling. Power of a randomization test in a single case multiple baseline AB design. *PLoS ONE*, 15(2):e0228355, February 2020.
- [5] Rasmus Bro and Age K. Smilde. Principal component analysis. *Analytical Methods*, 6(9):2812–2831, 2014.
- [6] Isis Bulté and Patrick Onghena. The Single-Case Data Analysis Package: Analysing Single-Case Experiments with R Software. *Journal of Modern Applied Statistical Methods*, 12(2):450–478, November 2013.
- [7] Michael D. Ernst. Permutation Methods: A Basis for Exact Inference. *Statistical Science*, 19(4), November 2004.
- [8] Jingjing Fu, Shuheng Liu, Siqi Du, Siqiao Ruan, Xuliang Guo, Weiwei Pan, Abhishek Sharma, and Stefan Konigorski. Multimodal N-of-1 trials: A Novel Personalized Healthcare Design, February 2023.
- [9] Ian Goodfellow, Yoshua Bengio, and Aaron Courville. *Deep Learning*. MIT Press, 2016. <http://www.deeplearningbook.org>.
- [10] Tanya Graham, Sangeeta Sooriah, Rachel Box, Heather Gage, Peter Williams, Victoria Clemett, and Patricia Grocott. Participatory co-design of patient-reported outcome indicators and N-of-1 evaluation of a dressing glove for Epidermolysis bullosa. *Journal of Wound Care*, 29(12):751–762, December 2020.
- [11] Nobukazu Hayashi, Hirohiko Akamatsu, Makoto Kawashima, and Acne Study Group. Establishment of grading criteria for acne severity. *The Journal of Dermatology*, 35(5):255–260, 2008.

- [12] Mieke Heyvaert and Patrick Onghena. Randomization tests for single-case experiments: State of the art, state of the science, and state of the application. *Journal of Contextual Behavioral Science*, 3(1):51–64, January 2014.
- [13] Ian T. Jolliffe and Jorge Cadima. Principal component analysis: A review and recent developments. *Philosophical transactions. Series A, Mathematical, physical, and engineering sciences*, 374(2065):20150202, April 2016.
- [14] Matthias Kirchler, Shahryar Khorasani, Marius Kloft, and Christoph Lippert. Two-sample testing using deep learning. In Silvia Chiappa and Roberto Calandra, editors, *Proceedings of the Twenty Third International Conference on Artificial Intelligence and Statistics*, volume 108 of *Proceedings of Machine Learning Research*, pages 1387–1398. PMLR, 26–28 Aug 2020.
- [15] S. Koide, N. R. Smoll, J. Liew, K. Smith, A. Rizzitelli, M. W. Findlay, and D. J. Hunter-Smith. A randomized ‘N-of-1’ single blinded clinical trial of barbed dermal sutures vs. smooth sutures in elective plastic surgery shows differences in scar appearance two-years post-operatively. *Journal of Plastic, Reconstructive & Aesthetic Surgery*, 68(7):1003–1009, July 2015.
- [16] Mark A. Kramer. Nonlinear principal component analysis using autoassociative neural networks. *AIChE Journal*, 37(2):233–243, 1991.
- [17] Pi-I. D. Lin, Chia-Fang Wu, Hwang-Shang Kou, Tzu-Ying Huang, Jentaie Shiea, and Ming-Tsang Wu. Removal of Diethylhexyl Phthalate from Hands by Handwashing: Evidence from Experimental N-of-1 and Crossover Designs. *Scientific Reports*, 7(1):454, March 2017.
- [18] Rd Mirza, S Punja, S Vohra, and G Guyatt. The history and development of N-of-1 trials. *Journal of the Royal Society of Medicine*, 110(8):330–340, August 2017.
- [19] Patrick Onghena. Randomization Tests or Permutation Tests? A Historical and Terminological Clarification. pages 209–227. January 2018.
- [20] Patrick Onghena and Eugene S. Edgington. Randomization tests for restricted alternating treatments designs. *Behaviour Research and Therapy*, 32:783–786, 1994.
- [21] Adam Paszke, Sam Gross, Francisco Massa, Adam Lerer, James Bradbury, Gregory Chanan, Trevor Killeen, Zeming Lin, Natalia Gimelshein, Luca Antiga, Alban Desmaison, Andreas Kopf, Edward Yang, Zachary DeVito, Martin Raison, Alykhan Tejani, Sasank Chilamkurthy, Benoit Steiner, Lu Fang, Junjie Bai, and Soumith Chintala. Pytorch: An imperative style, high-performance deep learning library. In *Advances in Neural Information Processing Systems 32*, pages 8024–8035. Curran Associates, Inc., 2019.
- [22] F. Pedregosa, G. Varoquaux, A. Gramfort, V. Michel, B. Thirion, O. Grisel, M. Blondel, P. Prettenhofer, R. Weiss, V. Dubourg, J. Vanderplas, A. Passos, D. Cournapeau, M. Brucher, M. Perrot, and E. Duchesnay. Scikit-learn: Machine learning in Python. *Journal of Machine Learning Research*, 12:2825–2830, 2011.
- [23] José Pinheiro, Douglas Bates, and R Core Team. *nlme: Linear and Nonlinear Mixed Effects Models*, 2023. R package version 3.1-163.
- [24] Sebastian Raschka. Mlxtend: Providing machine learning and data science utilities and extensions to python’s scientific computing stack. *The Journal of Open Source Software*, 3(24), April 2018.
- [25] Kravitz Rl, Gabler Nb, Kaplan Hc, Kravitz Rl, Larson Eb, Pace Wd, and Schmid Ch. Design and Implementation of N-of-1 Trials: A User’s Guide.
- [26] Matthieu Roustit, Joris Gai, Olivier Gaget, Charles Khouri, Myriam Mouhib, Adrien Lotito, Sophie Blaise, Christophe Seinturier, Fabien Subtil, Adeline Paris, Claire Cracowski, Bernard Imbert, Patrick Carpentier, Sunita Vohra, and Jean-Luc Cracowski. On-Demand Sildenafil as a Treatment for Raynaud Phenomenon. *Annals of Internal Medicine*, 169(10):694–703, November 2018.
- [27] Jonathan A Shaffer, Ian M Kronish, Louise Falzon, Ying Kuen Cheung, and Karina W Davidson. N-of-1 Randomized Intervention Trials in Health Psychology: A Systematic Review and Methodology Critique. *Annals of Behavioral Medicine*, 52(9):731–742, August 2018.
- [28] Jerry KL Tan. Current measures for the evaluation of acne severity. *Expert Review of Dermatology*, 3(5):595–603, October 2008.
- [29] Pauli Virtanen, Ralf Gommers, Travis E. Oliphant, Matt Haberland, Tyler Reddy, David Cournapeau, Evgeni Burovski, Pearu Peterson, Warren Weckesser, Jonathan Bright, Stéfan J. van der Walt, Matthew Brett, Joshua Wilson, K. Jarrod Millman, Nikolay Mayorov, Andrew R. J. Nelson, Eric Jones, Robert Kern, Eric Larson, C J Carey, Ilhan Polat, Yu Feng, Eric W. Moore, Jake VanderPlas, Denis Laxalde, Josef Perktold, Robert Cimrman, Ian Henriksen, E. A. Quintero, Charles R. Harris, Anne M. Archibald, Antônio H. Ribeiro, Fabian Pedregosa, Paul van Mulbregt, and SciPy 1.0 Contributors. SciPy 1.0: Fundamental Algorithms for Scientific Computing in Python. *Nature Methods*, 17:261–272, 2020.